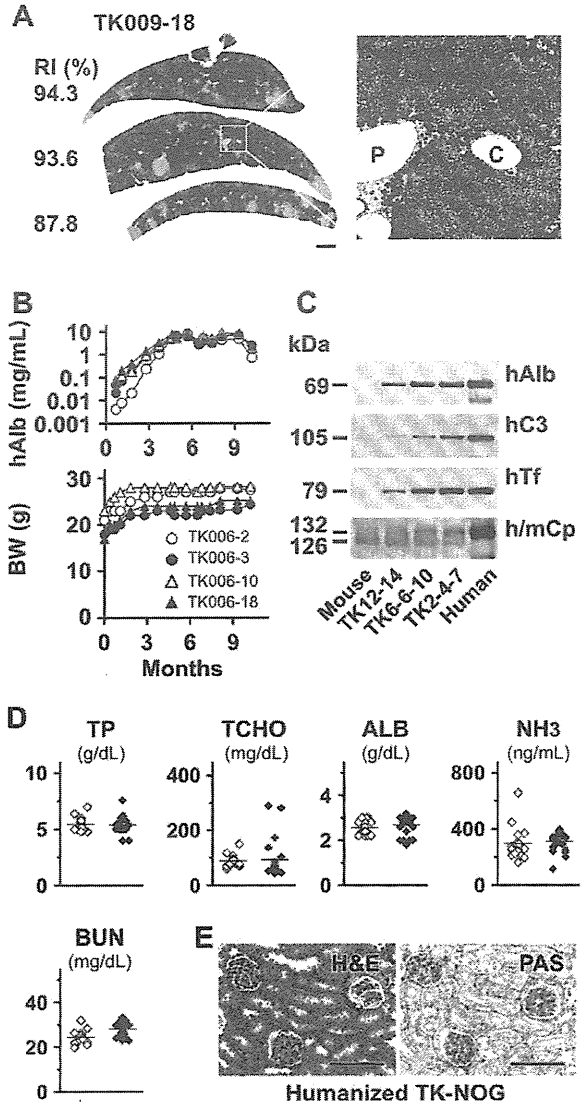

Fig. 1. (A) Reconstituted 'humanized liver' in TK-NOG mouse. Immunohistochemical staining of sections obtained from TK009-18 liver using h-CK8/18 antibody. The RI (%) for each section is indicated. Scale bar: 1 mm. An enlarged view of the boxed area is shown in the inset right. P, portal tract; C, central vein. (B) The human albumin (hAlb) level in the plasma of four TK-NOG mice and their body weight (BW) was measured over a 9-month period after GCV conditioning and human liver cell transplantation. (C) Immunoblot analyses of sera from three humanized TK-NOG mice with antibodies for specific for human albumin (hAlb), complement C3 proteins (hC3), transferrin (hTF), and for human and mouse ceruloplasmin (h/mCp). The RI of these mice (TK12-14, 6-6-10, and 2-4-7) mice were approximately 10%, 30%, and 85%, respectively. (D) Comparison of total protein (TP), total cholesterol (TCHO), albumin (ALB), ammonia (NH_3), and serum blood urea nitrogen (BUN) levels between the control NOG and humanized TK-NOG mice. The hAlb level in all of the humanized mice is >3 mg/mL. Open rhomboid, control NOG mice; filled rhomboid, humanized TK-NOG mice. (E) H&E and PAS staining of kidney obtained from a humanized TK-NOG mouse (hAlb > 5.0 mg/mL). Scale bars: 100 μm.

using uPA-dependent models. The *Fah*$^{-/-}$ model could provide a more stable humanization model; Bissig et al. achieved a long-term (34 weeks) reconstitution of *Fah*$^{-/-}$ mice as an experimental model for hepatitis C virus treatment [4]. However, long-term maintenance of these mice required repeated cycles of exposure to a drug (NTBC; 2-(2-nitro-4-trifluoro-methylbenzoyl)-1,3-cyclohexanedione) to prevent hepatocellular carcinomas, which will develop from the remaining mouse hepatocytes [4].

Serum proteins were analyzed in detail in three humanized TK-NOG mice by immunoblot analysis. Multiple different human proteins (albumin, complement C3, transferrin, and ceruloplasmin) were detected in their sera (Fig. 1C). The presence of the 105 kDa human C3 α chain in serum was of interest, since it indicates that the C3 precursor protein was processed by C3 convertase [16]. Although a high serum concentration of human C3 was thought to contribute to the renal failure that develops in uPA transgenic mice [5], humanized TK-NOG mice did not develop any biochemical or histologic evidence of kidney failure (Fig. 1D and E). Measurement of the serum total protein (TP), total cholesterol (TCHO), albumin (ALB), and ammonia (NH_3) indicated that the humanized liver had normal synthetic and metabolic function (Fig. 1D).

We further examined the histology of the humanized TK-NOG liver. In hematoxylin and eosin (H&E) stained sections, the human hepatocytes (HLA, ASGR1 and human albumin-positive) could be clearly distinguished by their size and pale cytoplasm from mouse hepatocytes (Fig. 2A), which is consistent with previous descriptions [11,17]. Periodic acid-Schiff (PAS) staining revealed that glycogen accumulation was restricted to the cytoplasm of the human hepatocytes. Most human hepatocytes (h-CK8/18-positive) were present as small foci that appeared to grow by clonal expansion within host parenchyma within 6 weeks after transplantation. There is a possibility that the reconstituted liver could be derived from a fusion between human and mouse hepatocytes [18]. However, double-immunofluorescent staining with antibodies specific for human or mouse albumin as well as PCR analysis of genomic segments within tissues isolated by laser-capture microdissection indicated that there was no evidence for fusion events between mouse and human cells (Fig. S4).

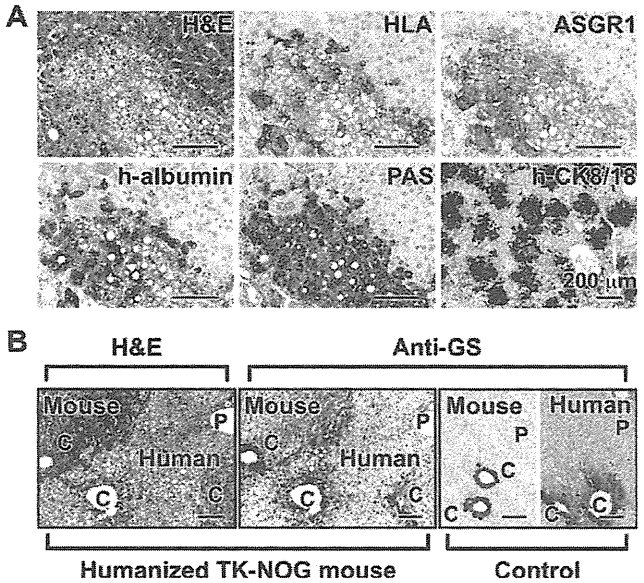

Fig. 2. (A) Histology and immunohistochemistry of the liver of humanized TK-NOG mice. Serial liver sections were stained for H&E, HLA, ASGR1, h-albumin, PAS, and h-CK8/18. Scale bars: 100 μm. (B) The position-specific pattern of GS expression within the liver lobule. H&E and immunohistochemical staining with anti-GS antibody in liver sections obtained from humanized TK-NOG mice 14 weeks after transplantation of human liver cells. The 'Mouse' and 'Human' hepatocyte boundary is indicated by a dashed line in the images on the left. Liver sections from control NOG or human liver sections that were stained with the anti-GS antibody are shown on the right. Scale bars: 100 μm. P, portal tract; C, central vein.

3.2. The gene expression profile in reconstituted TK-NOG liver resembles human liver

We also evaluated global gene expression patterns in humanized TK-NOG liver using microarrays. There was a very high level of correlation between the gene expression profiles in TK-NOG humanized liver tissue and that in the transplanted donor human liver cells ($r^2 = 0.7219$; Fig. 3A). There was only a minimal level (8%) of probes on the human gene expression array that cross-hybridized with murine mRNA (Fig. S5A). Since these mice could be used to evaluate drug metabolism, the level of expression of 26 drug metabolism-related mRNAs were also evaluated by quantitative PCR (qPCR) analyses, including: 12 CYP450 and two phase II enzymes, five SLC, and four ABC transporters, and three nuclear hormone receptors. All of the mRNAs that were expressed in donor liver cells were reproducibly expressed at comparable levels in the livers obtained from four humanized TK-NOG mice (Fig. 3B). The microarray and qPCR results were highly correlated ($r^2 = 0.9784$; Fig. S5B). In addition, there was abundant expression of human CYP3A4 in the liver of humanized TK-NOG mice (Fig. S6).

3.3. Functional analyses of the reconstituted 'humanized liver' in TK-NOG mice

We also investigated whether the reconstituted 'humanized liver' had the three-dimensional architecture characteristic of mature human liver. Since glutamine synthetase (GS) is normally expressed within a narrow zone around the central vein of the liver lobule [19], its pattern of expression in control NOG and in humanized TK-NOG livers was examined. There was no evidence for zonal GS expression within liver lobules containing human hepatocytes 6 weeks after transplantation, which suggested an immature lobular organization at this time (data not shown). In contrast, at 14 weeks after transplantation, GS had pericentral expression in the human-derived regions of the reconstituted TK-NOG liver (Fig. 2B). Thus, after 14 weeks, a mature hepatic architecture is formed in the reconstituted humanized liver in TK-NOG mice, which is in agreement with prior studies indicating that zonation occurs 8 weeks after autologous liver cell transplantation [20].

To determine whether human-specific drug metabolism could occur in the humanized TK-NOG liver, we measured the metabolism of debrisoquine (DEB), a prototypical CYP2D6 substrate that is converted to its 4-OH metabolite (4-OH DEB) by *CYP2D6*. Since mice are relatively deficient in this activity [21], an increase of 4-OH DEB production indicates that human (CYP2D6-mediated) drug metabolism is occurring in the humanized liver. A single oral dose of DEB (2.0 mg/kg) was administered to control NOG and to humanized TK-NOG mice (>4.5 mg/mL hAlb), and the amount of DEB and 4-OH DEB in serum was measured as a function of time after dosing (Fig. 3C). The area under the plasma concentration–time curve (AUC) for DEB showed no significant difference between humanized TK-NOG ($n = 6$) and NOG ($n = 9$) mice

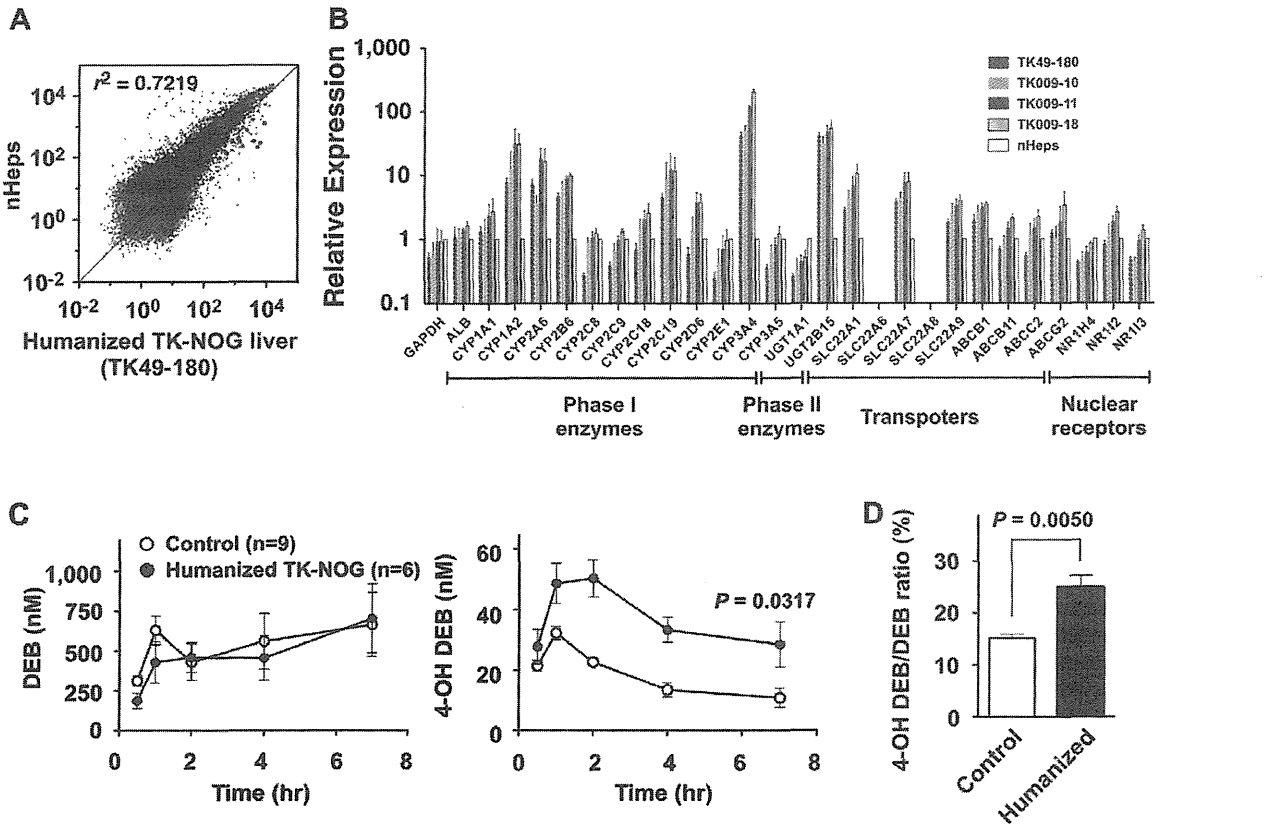

Fig. 3. (A) Gene expression within the reconstituted 'humanized liver' of TK-NOG mice. Global gene expression profiles within a fully humanized TK-NOG liver (RI of >85%) and donor human liver cells were compared by microarray analysis. The blue and black triangles indicate 'absent or marginal' and 'present' detection calls, respectively. The red circles indicate the probe sets for mRNAs related to drug metabolism. (B) The relative expression of 26 human drug metabolism related mRNAs in four independent 'humanized' TK-NOG livers and in donor human liver cells (nHeps) was assessed by qPCR. Each bar represents the average of three independent determinations and the standard error is shown. (C) Human (CYP2D6)-specific drug biotransformation in humanized TK-NOG mice. The serum concentration of DEB (left panel) and 4-OH DEB (right panel) in control NOG ($n = 9$) and humanized TK-NOG ($n = 6$) mice were measured 0, 0.5, 1, 2, 4, and 7 h after administration of a single oral dose of DEB (2 mg/kg). Each data point represents the average ± SD of 6–9 independent mice tested. (D) Urine samples were collected between 0 and 7 h after DEB administration. The % ratio of 4-OH DEB/DEB excreted into urine within 7 h was compared between control NOG ($n = 9$) and humanized TK-NOG mice ($n = 6$). By all of these measures, humanized TK-NOG mice had significantly increased amounts of 4-OH DEB in the plasma and higher 4-OH DEB excretion than control NOG mice.

(3211 ± 524.1 and 3587 ± 854.0 nM·h, respectively; $p = 0.7139$). However, humanized TK-NOG mice had significantly increased amounts of 4-OH DEB in their sera, the AUC for 4-OH DEB was 2.2-fold higher in humanized TK-NOG mice than in NOG mice (247.7 ± 26.7 and 112.9 ± 12.6 nM·h, respectively; $p = 0.0028$). Consistent with this difference, an increased amount of the 4-OH DEB metabolite was excreted into the urine of humanized TK-NOG mice (Fig. 3D). These results indicate that the humanized liver can mediate a human CYP2D6-specific drug biotransformation.

4. Discussion

The molecular, histological and functional studies demonstrate that the reconstituted 'humanized liver' in TK-NOG mice is a mature and functional "human organ". Because of these unique properties, we believe that this model could become a preferred platform for studying many aspects of human liver physiology. A unique advantage is that the TK-NOG humanized liver and its synthetic function could be stably maintained for a long period after transplantation, without the use of exogenous drugs. The TK-NOG mice did not develop systemic morbidity (liver disease, renal disease, and bleeding diathesis), nor were drug treatments required to suppress the liver tumor development. This has not previously been achieved by any of the other (uPA and *Fah*$^{-/-}$) liver reconstitution models. The longer survival and stable humanization pattern in TK-NOG mice provides a wide time-window that facilitates drug metabolism, toxicology or other longer-term studies. In fact, their prolonged survival has enabled us to 're-use' mice in different studies.

CYP3A4 is the most abundant CYP450 enzyme in human liver, and it is able to metabolize nearly 50% of all marketed drugs [22]. The metabolism of ~30% and ~10% of marketed drugs is mediated by CYP2D6 and CYP2C19, respectively [23]. We have demonstrated that reconstituted TK-NOG mice can carry out a human-specific (CYP2D6-mediated) biotransformation of a test drug. Furthermore, a large number of human phase I and II enzymes, transporters, and nuclear receptors also expressed in the humanized TK-NOG liver. The murine organs mediate many important extra-hepatic components of drug clearance (renal clearance, intestinal absorption, and metabolism, etc.) in this model system. Nevertheless, this data indicates that the humanized liver in TK-NOG mice holds great promise as a model system for studying the hepatic component of human drug metabolism. The ability to maintain these mice for prolonged time periods without requiring maintenance drugs indicates that these mice could be especially valuable for toxicological studies that require a prolonged period of drug administration.

The TK-NOG model also has another unique advantage; additional GCV doses can be administered after human cells have repopulated the liver. This enables a 'mop up' strategy to be developed to ablate residual mouse hepatic cells after human cell reconstitution, which could ensure that a very high level of human replacement is reproducibly achieved.

Acknowledgments

We thank Dr. R.D. Palmiter for providing the plasmid p2335A-1 containing the mouse albumin enhancer/promoter gene, and M. Kuronuma, S. Inoue, Y. Ando, N. Ogata, T. Mizushima, E. Hayakawa, K. Hioki, T. Sugioka, T. Ogura, T. Kamisako, and T. Etoh for outstanding technical assistance with the animal experiments. We thank C. Yagihashi and N. Omi for technical assistance with molecular analyses, and Drs. M. Kajimura, M. Ohmura, and Y. Ohnishi for helpful discussions. This work was supported by a Grant-in-Aid for Scientific Research (17300136 and 21240042) to H.S. Design of metabolome analysis in humanized NOG mice was supported by Research and Development of the Next-Generation Integrated Simulation of Living Matter, a part of the Development and Use of the Next-Generation Supercomputer Project of MEXT. M.S. is supported by JST, ERATO, Suematsu Gas Biology Project, Tokyo 160-8582, Japan. G.P. was supported by funding from a transformative RO1 award (1R01DK090992-01) from the NIDDK.

Appendix A. Supplementary data

Supplementary data associated with this article can be found, in the online version, at doi:10.1016/j.bbrc.2011.01.042.

References

[1] H. Suemizu, M. Hasegawa, K. Kawai, K. Taniguchi, M. Monnai, M. Wakui, M. Suematsu, M. Ito, G. Peltz, M. Nakamura, Establishment of a humanized model of liver using NOD/Shi-scid IL2Rg(null) mice, Biochem. Biophys. Res. Commun. 377 (2008) 248–252.
[2] M. Dandri, M.R. Burda, E. Torok, J.M. Pollok, A. Iwanska, G. Sommer, X. Rogiers, C.E. Rogler, S. Gupta, H. Will, H. Greten, J. Petersen, Repopulation of mouse liver with human hepatocytes and in vivo infection with hepatitis B virus, Hepatology 33 (2001) 981–988.
[3] D.F. Mercer, D.E. Schiller, J.F. Elliott, D.N. Douglas, C. Hao, A. Rinfret, W.R. Addison, K.P. Fischer, T.A. Churchill, J.R. Lakey, D.L. Tyrrell, N.M. Kneteman, Hepatitis C virus replication in mice with chimeric human livers, Nat. Med. 7 (2001) 927–933.
[4] K.D. Bissig, S.F. Wieland, P. Tran, M. Isogawa, T.T. Le, F.V. Chisari, I.M. Verma, Human liver chimeric mice provide a model for hepatitis B and C virus infection and treatment, J. Clin. Invest. 120 (2010) 924–930.
[5] C. Tateno, Y. Yoshizane, N. Saito, M. Kataoka, R. Utoh, C. Yamasaki, A. Tachibana, Y. Soeno, K. Asahina, H. Hino, T. Asahara, T. Yokoi, T. Furukawa, K. Yoshizato, Near completely humanized liver in mice shows human-type metabolic responses to drugs, Am. J. Pathol. 165 (2004) 901–912.
[6] M. Katoh, T. Sawada, Y. Soeno, M. Nakajima, C. Tateno, K. Yoshizato, T. Yokoi, In vivo drug metabolism model for human cytochrome P450 enzyme using chimeric mice with humanized liver, J. Pharm. Sci. 96 (2007) 428–437.
[7] L. Lootens, P. Van Eenoo, P. Meuleman, G. Leroux-Roels, F.T. Delbeke, The uPA(+/+)-SCID mouse with humanized liver as a model for in vivo metabolism of 4-androstene-3, 17-dione, Drug Metab. Dispos. 37 (2009) 2367–2374.
[8] M. Zhao, S.A. Amiel, S. Ajami, J. Jiang, M. Rela, N. Heaton, G.C. Huang, Amelioration of streptozotocin-induced diabetes in mice with cells derived from human marrow stromal cells, PLoS One 3 (2008) e2666.
[9] O.J. Pozo, P. Van Eenoo, K. Deventer, L. Lootens, S. Grimalt, J.V. Sancho, F. Hernandez, P. Meuleman, G. Leroux-Roels, F.T. Delbeke, Detection and structural investigation of metabolites of stanozolol in human urine by liquid chromatography tandem mass spectrometry, Steroids 74 (2009) 837–852.
[10] H. Kamimura, N. Nakada, K. Suzuki, A. Mera, K. Souda, Y. Murakami, K. Tanaka, T. Iwatsubo, A. Kawamura, T. Usui, Assessment of chimeric mice with humanized liver as a tool for predicting circulating human metabolites, Drug Metab. Pharmacokinet. 25 (2010) 223–235.
[11] H. Azuma, N. Paulk, A. Ranade, C. Dorrell, M. Al-Dhalimy, E. Ellis, S. Strom, M.A. Kay, M. Finegold, M. Grompe, Robust expansion of human hepatocytes in Fah-/-/Rag2-/-/Il2rg-/- mice, Nat. Biotechnol. 25 (2007) 903–910.
[12] R.A. Heyman, E. Borrelli, J. Lesley, D. Anderson, D.D. Richman, S.M. Baird, R. Hyman, R.M. Evans, Thymidine kinase obliteration: creation of transgenic mice with controlled immune deficiency, Proc. Natl. Acad. Sci. USA 86 (1989) 2698–2702.
[13] E. Borrelli, R. Heyman, C. Arias, P. Sawchenko, R. Evans, Transgenic mice with inducible dwarfism, Nature 339 (1989) 538–541.
[14] Y. Zhang, S.Z. Huang, S. Wang, Y.T. Zeng, Development of an HSV-tk transgenic mouse model for study of liver damage, FEBS J. 272 (2005) 2207–2215.
[15] M. Ito, H. Hiramatsu, K. Kobayashi, K. Suzue, M. Kawahata, K. Hioki, Y. Ueyama, Y. Koyanagi, K. Sugamura, K. Tsuji, T. Heike, T. Nakahata, NOD/SCID/gamma(c)(null) mouse: an excellent recipient mouse model for engraftment of human cells, Blood 100 (2002) 3175–3182.
[16] V.A. Bokisch, M.P. Dierich, H.J. Muller-Eberhard, Third component of complement (C3): structural properties in relation to functions, Proc. Natl. Acad. Sci. USA 72 (1975) 1989–1993.
[17] P. Meuleman, L. Libbrecht, R. De Vos, B. De Hemptinne, K. Gevaert, J. Vandekerckhove, T. Roskams, G. Leroux-Roels, Morphological and biochemical characterization of a human liver in a uPA-SCID mouse chimera, Hepatology 41 (2005) 847–856.
[18] H. Fujino, H. Hiramatsu, A. Tsuchiya, A. Niwa, H. Noma, M. Shiota, K. Umeda, M. Yoshimoto, M. Ito, T. Heike, T. Nakahata, Human cord blood CD34+ cells develop into hepatocytes in the livers of NOD/SCID/gamma(c)null mice through cell fusion, FASEB J. 21 (2007) 3499–3510.
[19] R. Gebhardt, D. Mecke, Heterogeneous distribution of glutamine synthetase among rat liver parenchymal cells in situ and in primary culture, EMBO J. 2 (1983) 567–570.

[20] K.M. Braun, J.L. Degen, E.P. Sandgren, Hepatocyte transplantation in a model of toxin-induced liver disease: variable therapeutic effect during replacement of damaged parenchyma by donor cells, Nat. Med. 6 (2000) 320–326.
[21] Y. Masubuchi, T. Iwasa, S. Hosokawa, T. Suzuki, T. Horie, S. Imaoka, Y. Funae, S. Narimatsu, Selective deficiency of debrisoquine 4-hydroxylase activity in mouse liver microsomes, J. Pharmacol. Exp. Ther. 282 (1997) 1435–1441.
[22] S. Rendic, Summary of information on human CYP enzymes: human P450 metabolism data, Drug Metab. Rev. 34 (2002) 83–448.
[23] R. Zuber, E. Anzenbacherova, P. Anzenbacher, Cytochromes P450 and experimental models of drug metabolism, J. Cell Mol. Med. 6 (2002) 189–198.